Propulsion and Power Research 2013;2(3):214–224

http://ppr.buaa.edu.cn/

Propulsion and Power Research

www.sciencedirect.com

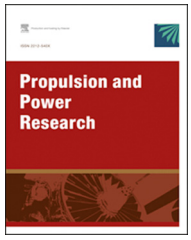

ORIGINAL ARTICLE

Comparative performance analysis of combined-cycle pulse detonation turbofan engines (PDTEs)

Sudip Bhattrai, Hao Tang*

Nanjing University of Aeronautics and Astronautics, Nanjing, Jiangsu 210016, China

Received 9 November 2012; accepted 18 March 2013
Available online 17 August 2013

KEYWORDS

Single-stage-to-orbit (SSTO);
Afterburners;
Integrated propulsion systems;
Turbine-based combined-cycle (TBCC);
Rocket-based combined-cycle (RBCC)

Abstract Combined-cycle pulse detonation engines are promising contenders for hypersonic propulsion systems. In the present study, design and propulsive performance analysis of combined-cycle pulse detonation turbofan engines (PDTEs) is presented. Analysis is done with respect to Mach number at two consecutive modes of operation: (1) Combined-cycle PDTE using a pulse detonation afterburner mode (PDA-mode) and (2) combined-cycle PDTE in pulse detonation ramjet engine mode (PDRE-mode). The performance of combined-cycle PDTEs is compared with baseline afterburning turbofan and ramjet engines. The comparison of afterburning modes is done for Mach numbers from 0 to 3 at 15.24 km altitude conditions, while that of pulse detonation ramjet engine (PDRE) is done for Mach 1.5 to Mach 6 at 18.3 km altitude conditions. The analysis shows that the propulsive performance of a turbine engine can be greatly improved by replacing the conventional afterburner with a pulse detonation afterburner (PDA). The PDRE also outperforms its ramjet counterpart at all flight conditions considered herein. The gains obtained are outstanding for both the combined-cycle PDTE modes compared to baseline turbofan and ramjet engines.

1. Introduction

Pulse detonation engine (PDE) is an air-breathing intermittent combustion engine in which detonations at high frequencies are driven through a tube, simultaneously burning and accelerating the fuel-air mixture to create thrust. PDEs are currently attracting considerable attention because they promise performance improvements over

*Corresponding author: Tel.: +86 13912988530.
E-mail address: hao.tang@nuaa.edu.cn (Hao Tang).

Peer review under responsibility of National Laboratory for Aeronautics and Astronautics, China.

ELSEVIER Production and hosting by Elsevier

2212-540X © 2013 National Laboratory for Aeronautics and Astronautics. Production and hosting by Elsevier B.V. All rights reserved.
http://dx.doi.org/10.1016/j.jppr.2013.04.007

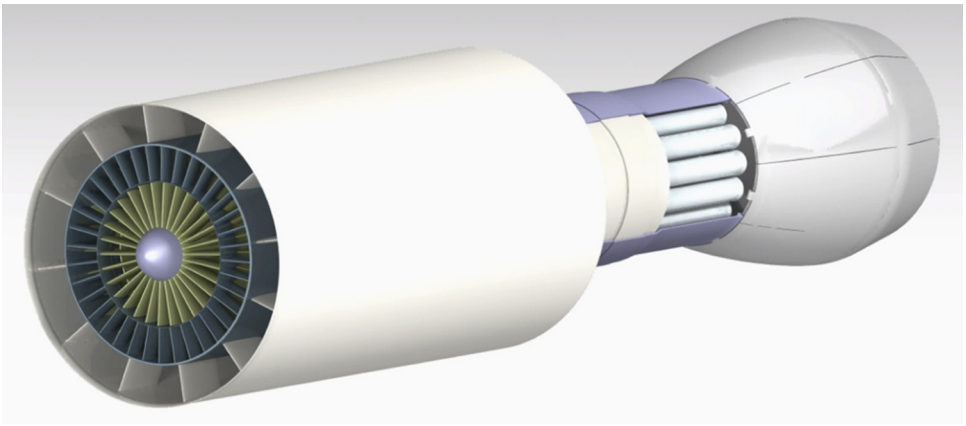

Figure 1 Conceptual model of the combined-cycle PDTE analyzed in this study.

existing air-breathing propulsion devices, especially at low fight Mach numbers [1,2]. During the past 60 years or so, there have been numerous research efforts at harnessing the potential of detonations for propulsion applications [3].

Recently, more advanced concepts have been studied, such as integrated PDEs that use pulsed detonation combustor (PDC) incorporated into a gas-turbine engine as the primary combustion system, with the intention of increasing efficiency by utilizing the strengths of both engines [4]. The studies about integrated PDEs have also been related to the performance analysis of gas-turbine engine with a pulse detonation afterburner (PDA), in which PDA is integrated into a baseline gas-turbine, hence, replacing the conventional deflagration afterburners [5,6]. It was shown that the pulse detonation turbofan engine (PDTE) concept would have superior performance for an operating frequency of 100 Hz and higher compared to the conventional afterburning turbofan engine. Another concept suggested the embodiment of PDC into the bypass duct of turbofan engines for thrust augmentation in place of afterburners [7]. In these studies, integrated PDEs have shown possibilities of obtaining a more efficient engine by the replacements of conventional core combustor and afterburner with PDC [8].

The embodiment of PDE into combined-cycle turbojet engines that can operate in variable operation modes enabling aircrafts to fly at wider ranges of speeds, altitudes and environmental conditions was the subject of a series of recent studies by Johnson et al. [9–11]. At conceptual level, the combined-cycle PDTE is a combination of two or more modes of operation, where a PDE is embodied into a baseline turbofan/turbojet engine. So far, studies related to the combined-cycle PDTEs have mostly been limited to conceptual levels only. In spite of the progress made to date, there still remains a major concern about the propulsive performance of combined-cycle PDTEs, especially in comparison with such well-established propulsion systems as ramjet and gas-turbine engines.

The objective of the present study is to research combined-cycle PDTE configurations, explain their operating principle and analyze the performance of an ideal combined-cycle PDTE at each mode of operation. The combined-cycle engine in this study uses a PDC embodied downstream of the mixer as an afterburner in the turbofan engine, and an auxiliary ram duct for direct ram air intake (Figure 1). The following performance comparisons are made for each combined-cycle engine operation modes to the baseline configurations:

(1) Performance comparison of baseline turbofan engine (with conventional afterburner) to the combined-cycle PDTE in PDA-mode where the PDC is used as afterburner for thrust augmentation.
(2) Performance comparison of baseline ramjet engine to the combined-cycle PDTE in pulse detonation ramjet engine mode (PDRE-mode) where the PDC operates directly on ram air.

The choice of gas-turbine engine in this study is a high bypass turbofan engine.

For flight operations from takeoff to approximately Mach 3, the main engine and an engine fan system provide airflow at a pressure and quantity used by the PDA for thrust augmentation. To maintain flight operations from supersonic speeds to hypersonic speeds of nearly 6, the core engine system is shut-down and ram air is introduced directly into the PDC by utilizing an auxiliary ram duct.

Pursuing the combined-cycle PDTE concept only makes sense if the comparison demonstrates comparative propulsive performance benefits. The present study provides a method for comparison of the performance of combined-cycle PDTE concept with conventional ramjet-based combined-cycle concept, i.e., the combined-cycle turbo-ramjet engine. The goal of this comparison is to show the prospects of combined-cycle PDTE for future applications in hypersonic, as well as in the initial phases of single-stage-to-orbit (SSTO) flights.

2. Combined-cycle PDTE design concepts

The combined-cycle PDTE concepts explore the alternative use of PDC as afterburner for thrust augmentation in

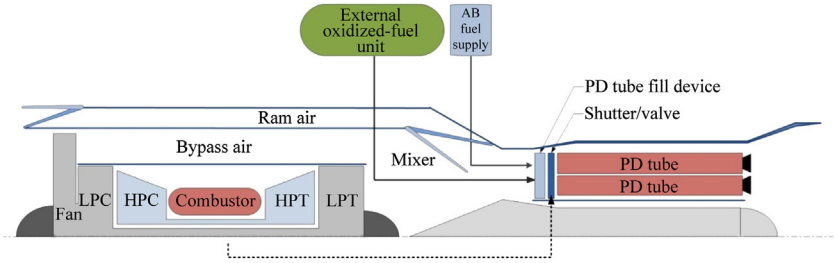

Figure 2 Combined-cycle turbofan engine using a PDA. (LPC-low pressure compressor; HPC-high pressure compressor; HPT-high pressure turbine; LPT-low pressure turbine; AB-afterburner.)

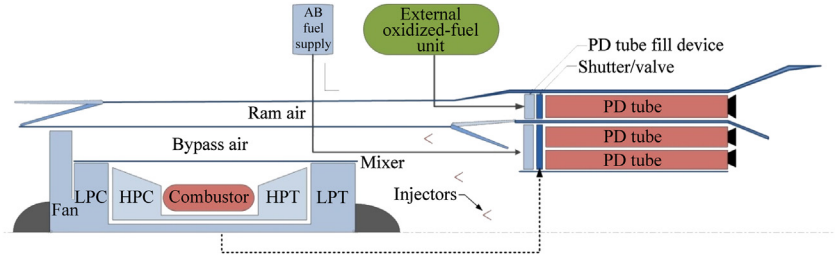

Figure 3 Combined-cycle PDTE with mixed-type afterburner and preconditioning.

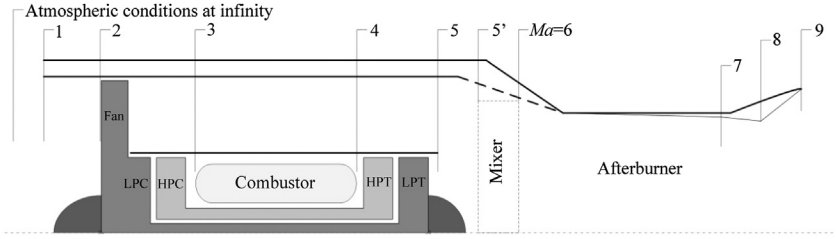

Figure 4 Schematic of the baseline turbofan engine with stage numbering.

a turbofan engine and in an entirely different mode of operation, as a fully operational PDRE for thrust generation. In this study two new combined-cycle PDTE concepts are presented as follows:

2.1. Combined-cycle turbofan engine using a PDA

In this concept of combined-cycle PDTE, shown in Figure 2, PDC is disposed downstream of the core engine, an auxiliary ram duct and ram-air valve system. During operation in PDA-mode, PDC receives core engine combustion gases as well as supplementary amount of ram air. The pulse detonation (PD) tube fill device fills the detonation tubes with incoming mixed flow and added fuel, while the shutter (coupled with low-pressure spool through a gear-train) controls the detonation frequency. The detonation products are mixed and expanded through the nozzle to create the net engine thrust. At higher supersonic Mach numbers, the core engine is either stalled or shut-down by rotating the fan blades to prevent air intake, and ram air is allowed to flow directly into the PDC hence enabling it to function independently as a PDRE.

2.2. Combined-cycle PDTE with mixed-type afterburners and preconditioning

The concept, shown in Figure 3, consists of circumferentially distributed concentric rings of PD tubes disposed in the mixed flow path. This concept differs from the earlier concept mainly in that the detonation tubes are circumferentially placed straight downstream of the ram duct as well, while the core afterburner space is occupied by conventional afterburner. Therefore, in contrast, the afterburner is a combination of pulse detonation and conventional deflagration afterburners, where the potential of both types can be utilized. Fuel can be added directly into either the core combustion gases (ram air entrance closed) or into the mixed ram air and core combustion gas flows (ram air entrance open). By controlling the passage of ram air only, the PDC can be operated without the use of conventional afterburners when required. That is, only the ram air passes into the PD tubes while the core flow is allowed to exit directly without afterburning. However, the core flow is mixed with PD tube flow at the nozzle hence contributing to the net thrust.

The injectors seen near the mixing section are required for this mixed-type afterburner operation. This process of injecting fuel into the core combustion products at temperatures below the ignition point is called *preconditioning*.

3. Analytical approach

The analytical calculations in the study have been performed using on-design cycle analysis program (ONX) [12] and MATLAB. The analysis particularly focuses on efficiency, specific impulse, thrust specific fuel consumption (TSFC) and specific thrust gains obtained by combined-cycle PDTE over conventional afterburning turbofan engine and pure ramjet engines. The analytical model for the computation of PDE performance parameters is referenced from the thermodynamic cycle analysis method for PDE given by Heiser et al. [13] and the PDE propulsive performance analysis model provided by Ma et al. [14]. Method for stage-wise analysis of ideal gas turbine engine can be referenced from any modern text book on aircraft propulsion, e.g., "aircraft propulsion" by Saeed Farokhi.

3.1. The baseline engine

The core engine selected for the analysis is the TF39-GE-1C high bypass turbofan engine, mainly because of its use in similar researches done earlier [4,15], which also made it easier to obtain complete set of the engine design parameters. The baseline engine, as shown in Figure 4, is

Table 1 TF39-G1-1C and the baseline models in ONX.

	Engine	
	TF39-GE-1C	Baseline model in ONX
Aircraft	C-5	N/A
Mach number	0	0
Altitude/km	0	15.24
Length/m	7.92	N/A
Weight/kg	3630	N/A
Max diameter/m	2.46	3
Frontal area/m^2	4.767	7.14
Ram duct area/m^2	–	2.38
Bypass ratio (BPR)	8	–
Fan pressure ratio (FPR)	1.56	1.56
Overall pressure ratio (OPR)	26	26
TSFC/(mg/N · s)	8.858	12.36
Max turbine inlet temperature/K	1561.112	1611.112

Table 3 Input parameters for baseline ramjet engine.

Input parameters	Values
Mach number (initial)	1.5
Reference altitude	18.3 km (60000 ft)
Reference temperature	216.667 K (390 R)
Reference pressure	7232 Pa (1.049 psi)
Back pressure ratio (p_0/p_9)	1
Max combustor exit temperature	1611.112 K (2900 R)
Inlet compressor sp. heat ratio	1.399
Nozzle entry sp. heat ratio	1.296
Fuel heating value (kerosene)	42.2 MJ/kg (18400 BTU/lbm)
Bleed air	1%
Diffuser pressure recovery (max)	0.995
Burner pressure recovery	0.96
Nozzle pressure recovery	0.985
Burner efficiency	0.995

Table 2 Input parameters for baseline turbofan engine.

Input parameters	Values	Input parameters	Values
Mach number (initial)	0	LPC polytropic efficiency	0.89
Reference altitude	15.24 km (50000 ft)	HPC polytropic efficiency	0.90
Reference temperature	216.667 K (390 R)	HPT polytropic efficiency	0.89
Reference pressure	11665.928 Pa (1.692 psi)	LPT polytropic efficiency	0.89
Turbine inlet temperature	1611.112 K (2900 R)	Burner efficiency	0.995
Compressor pressure ratio	26	Mech. shaft LP spool efficiency	0.99
LPC pressure ratio	1.56	Mech. shaft HP spool efficiency	0.99
Fan pressure ratio	1.56	Max turbine inlet temperature	1777.778 K (3200 R)
Back pressure ratio (p_0/p_9)	1	Turbine exit Mach number	0.5
Fuel heating value (kerosene)	42.2 MJ/kg (18400 BTU/lbm)	Max compressor pressure ratio	32
Bypass ratio	Floating values	Max pressure at burner inlet	4481.592 Pa (650 psi)
Compressor sp. heat ratio	1.3986	Max temperature at burner inlet	1033.334 K (1860 R)
Turbine sp. heat ratio	1.2957	Mach number at turbine exit	0.5
Bleed air	1%	Max % ref RPM-LP spool	110
Coolant air	5%	Max % ref RPM-HP spool	110
Burner pressure recovery	0.96	Afterburner pressure recovery	0.96
Nozzle pressure recovery	0.985	Afterburner efficiency	0.995
Diffuser max pressure recovery	0.995	Mixer pressure recovery (max)	0.97
Fan pressure ratio	0.98	Max temperature at afterburner outlet	2000 K (3600 R)
Fan polytropic efficiency	0.89	Afterburner sp. heat ratio	1.3

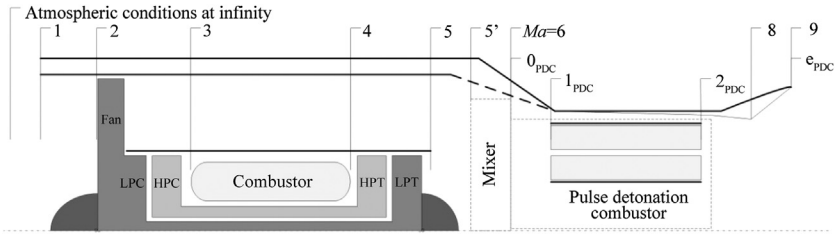

Figure 5 Schematic of combined-cycle PDTE with stage numbering.

derived from the TF39-GE-1C engine by accommodating a ram duct and an afterburner downstream of the core engine such that it receives the mixed air flow from the core engine and the bypass duct. Though the ram duct is not required for the baseline engine operation, it is necessary to emphasize the geometric similarity between the baseline and combined-cycle engines. The specifications for the baseline afterburner are taken from the default values given in ONX. The TF39-GE-1C engine parameters are referenced from Andrus [15], also from which the baseline engine parameters are derived. The model parameters for TF39-GE-1C and the baseline engine are listed in Table 1 for comparison.

3.1.1. *Baseline turbofan engine*

The baseline turbofan engine is the basic mode of the baseline engine that comprises a turbofan core engine coupled with a conventional afterburner. The performance of baseline engine was analyzed entirely in ONX, using the input parameters as given in Table 2. The Mach number is initialized with a value of 0 and the analysis extends up to Mach 3.

3.1.2. *Baseline ramjet engine*

The baseline ramjet engine comprises the ram duct (for direct air inflow), and the afterburner of the baseline engine used as the main combustor of the ramjet engine for subsonic-deflagration combustion. The baseline ramjet engine model was built in ONX based on the default ramjet model parameters given in ONX. Table 3 lists the input values used in the ONX program for analysis. The initial Mach number for ramjet engine is 1.5, and it is varied up to Mach 6 in the analysis.

3.2. *Analytical model of combined-cycle PDTE*

The combined-cycle PDTE configuration under analysis is as shown in Figure 5, which is also the conceptual model described in Section 2.1. It comprises a high-bypass turbofan engine coupled with an aft PDC, which is in fact the baseline engine with the conventional afterburner replaced by a PDC. This combined-cycle configuration is analyzed in MATLAB at two different operation modes, (1) a turbofan with PDA, and (2) a PDRE. The results are compared with respective baseline configurations, i.e., (1) turbofan with conventional afterburner, and (2) the ramjet engine. One simplification adopted in the analysis is the essential similarity between the PDA and PDRE operational mechanism, where the model parameters for detonation in both are the same, as given in Table 4. However, while the PDRE gets its intake airflow directly though the ram duct at high Mach numbers, the PDA operates at lower Mach regimes and relies on the core turbofan engine for its intake air.

Table 4 Model parameters for the detonation of stoichiometric hydrogen-air mixture.

Model parameters	Values
Atmospheric sp. heat ratio, γ_∞	1.4
Reactants sp. heat ratio, γ_1	1.3961
Products sp. heat ratio, γ_2	1.1653
Atmospheric gas constant, R_∞/(J/(kg · K))	287
Reactants gas constant, R_1/(J/(kg · K))	395.75
Products gas constant, R_2/(J/(kg · K))	346.2
Fuel heating value of the hydrogen fuel used for detonation, q/(J/kg)	5.4704×10^6
PDC inlet area, A_{in}/m^2	3.57
Pressure recovery at PDC inlet, σ	0.95
Fuel-to-air ratio in detonation tubes, f	0.0292

A total of 12 model parameters for the detonation of stoichiometric hydrogen air mixture are required in the analysis for each operation mode. Table 4 lists the values for 10 of the model parameters common to both the PDA and PDRE in the analysis. The other two model parameters in each cases are the inlet specific heat ratios (γ_0) and inlet gas constants (R_0). For PDA, these values are the assigned with the turbofan mixer outlet values γ_6 and R_6 respectively, which are mixer-outlet temperature dependent functions and have different values at different Mach numbers (mixer outlet stage is detonated as $Ma = 6$ in Figure 4 and Figure 5 by convention). While the values of γ_0 and R_0 for PDRE are the same as the atmospheric values γ_∞ and R_∞, since ram air is supplied directly in to the PDC.

For PDA, the mixer outflow properties are obtained from the ONX program and used in the MATLAB program as inputs (following a unit conversion). Ram air properties are essentially treated as the MATLAB inputs for PDC at PDRE-mode.

The PDC inflow conditions are defined using the total temperature T_{t1}, total pressure p_{t1}, and filling Mach number Ma_1. These PDC inlet values are obtained from the main engine mixer outlet values at PDA-mode and ram air values at PDRE-mode. The PDC inlet is a convergent-divergent type inlet where a total pressure recovery of 5% is assumed. Inlet throat area is controlled by using the area-Mach number relation. Ignoring the effect of inlet loss, the static temperature and pressure are obtained using isentropic relations for flow through the PDC inlet given by Eqs. (1) and (2). To ensure Chapman-Jouguet (CJ) properties for detonation products, the analytical CJ detonation Mach number, for the given heat release amount q, and reactant flow conditions, was imposed for products using Eq. (3).

$$T_1 = \frac{T_{t1}}{[1 + (\frac{\gamma_1 - 1}{2})Ma_1^2]} \tag{1}$$

$$p_1 = \frac{p_{t1}}{[1 + (\frac{\gamma_1 - 1}{2})Ma_1^2]^{\gamma_1/\gamma_1 - 1}} \tag{2}$$

$$Ma_d = \sqrt{\left(\frac{\gamma_2^2 - 1}{\gamma_1}\frac{q}{R_1 T_1} + \frac{\gamma_2^2 - \gamma_1}{\gamma_1^2 - \gamma_1}\right) + \sqrt{\left(\frac{\gamma_2^2 - 1}{\gamma_1}\frac{q}{R_1 T_1} + \frac{\gamma_2^2 - \gamma_1}{\gamma_1^2 - \gamma_1}\right)^2 - \left(\frac{\gamma_2}{\gamma_1}\right)^2}} \tag{3}$$

Here, T_1 and p_1 correspond to the PD tube filling conditions while the reactant and products model parameters-γ_1, γ_2, R_1 and q have values as given in Table 4. The corresponding temperature and pressure of detonation products are obtained using the relations in Eqs. (4) and (5).

$$\frac{p_2}{p_1} = \frac{1 + \gamma_1 Ma_d^2}{1 + \gamma_2} \tag{4}$$

$$\frac{T_2}{T_1} = \frac{R_1}{R_2}\frac{\gamma_2}{\gamma_1}\left[\frac{1 + \gamma_1 {Ma_d}^2}{(1 + \gamma_2)Ma_d^2}\right]^2 \tag{5}$$

The detonation tube exit conditions are obtained by assuming isentropic flow expansion from the CJ state of the detonation products to the exit plane which is assumed to be at ambient condition. The exit temperature is obtained using Eq. (6). The detonation tube exit values are calculated at the limiting case in which the effects of inlet loss and purge time are ignored. The thermodynamic cycle efficiency of an ideal PDE is given by Eq. (7).

$$T_e = T_2\left(\frac{p_\infty}{p_2}\right)^{\frac{\gamma_2 - 1}{\gamma_2}} \tag{6}$$

$$\eta_{th,PDE} = 1 - \frac{1}{q/c_{p\infty}T_\infty}\left[\frac{\gamma_\infty - 1}{\gamma_2 - 1}\frac{\gamma_2^2}{\gamma_\infty \gamma_1}\frac{R_1}{R_\infty}\frac{1}{Ma_d^2}\left(\frac{1 + \gamma_1 Ma_d^2}{1 + \gamma_2}\right)^{\frac{\gamma_2 + 1}{\gamma_2}} \times \left(\frac{T_1}{T_\infty}\right)^{1 - \frac{(\gamma_2 - 1)\gamma_\infty}{(\gamma_\infty - 1)\gamma_2}} - 1\right] \tag{7}$$

The exit velocity, given by Eq. (8), can be deduced by applying the energy balance between the PDC entrance and nozzle exit.

$$u_e = \sqrt{2[\eta_{th,PDE}q - (c_{p2}T_e - c_{p1}T_{t1})]} \tag{8}$$

Finally, the main propulsive performance parameters sp. thrust (F_{sp}), sp. impulse (I_{sp}), and TSFC, are obtained from Eqs. (9)–(11), respectively. For combined-cycle PDA-mode, the value of fuel-to-air ratio f should take into account for fuel used in turbofan core combustor.

$$F_{sp} = (1 + f)\sqrt{u_\infty^2 + 2[\eta_{th,PDE}q + (c_{p1} - c_{p\infty})T_1]} - u_\infty \tag{9}$$

$$I_{sp} = \frac{(1 + f)\sqrt{u_\infty^2 + 2[\eta_{th,PDE}q + (c_{p1} - c_{p\infty})T_1]} - u_\infty}{fg} \tag{10}$$

$$\text{TSFC} = \frac{f}{F_{sp}} \tag{11}$$

3.3. Analysis method

The analysis for this study has been schematically explained in the flow chart shown in Figure 6. The analysis was carried out in a step-wise manner as described below:

(1) The ONX program was used to obtain the performance of the baseline engines at Mach numbers from 0 to 3 at operating conditions corresponding to 15.24 km altitude for baseline turbofan engine and at Mach numbers from 1.5 to 6 at operating conditions corresponding to 18.3 km altitude for baseline ramjet engine. Also, in a separate calculation the baseline ramjet engine performance was calculated from Mach 0 to Mach 6 (the analysis is invalid above Mach 6) for specific impulse in ONX. The turbofan bypass ratio was allowed in ONX to adapt to a floating value depending upon the requirement at any Mach number.
(2) To compute the performance of the baseline turbofan engine with the afterburner replaced with PDA, the mixer outflow parameters of the core engine were obtained from ONX. These parameters were then used as inputs in MATLAB for the calculation of the overall performance of the turbofan engine with a PDA using the method and equations listed in Section 3.2. The range of the

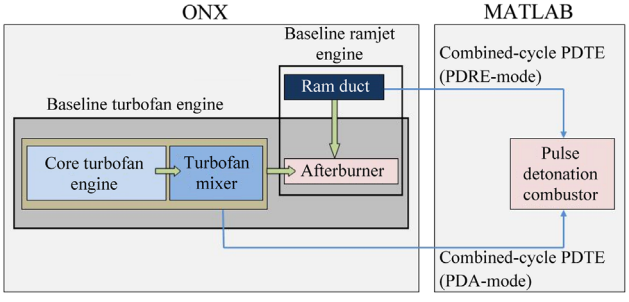

Figure 6 Analysis method flow chart.

calculation is from Mach 0 to Mach 3 for operating conditions of 15.24 km altitude. The calculation results obtained in this step, together with the results obtained for the baseline turbofan engine from step 1, provide a performance comparison between the baseline turbofan engine and the combined-cycle PDTE at PDA-mode.

(3) Since the PDRE takes the intake air through the ram duct of the combined-cycle engine, the performance calculation was done solely based on the MATLAB program. A simple model of analysis was adopted in which the PDRE receives ram air at atmospheric conditions. PDRE performance calculation was done from Mach 1.5 to Mach 6 at operating conditions of 18.3 km altitude, using the method and equations listed in Section 3.2. In a separate calculation the specific impulse was calculated from Mach 0 to Mach 11 to measure PDRE's theoretical operational range.

(4) The cycle efficiencies for ideal thermodynamic cycles for the baseline afterburner and ramjet engine (Brayton cycle), and for the PDA and PDRE (PDE cycle) were computed in the MATLAB. Also, since the Humphrey cycle is often cited as having similar performance to the PDE [12] the ideal Humphrey cycle efficiency was calculated, to check for its validity and comparison. The ideal Brayton and Humphrey cycle efficiencies are given by Eqs. (12) and (13), respectively.

$$\eta_{\text{th,Brayton}} = 1 - \frac{1}{q/c_{p\infty}T_\infty}\left[\frac{\gamma_1}{\gamma_\infty}\frac{\gamma_\infty - 1}{\gamma_1 - 1}\frac{R_1}{R_\infty}\left(\frac{q}{c_{p1}T_1}+1\right)\times\left(\frac{T_1}{T_\infty}\right)^{1-(\gamma_2-1)\gamma_\infty/(\gamma_\infty-1)\gamma_2} - 1\right] \tag{12}$$

$$\eta_{\text{th,Humphrey}} = 1 - \frac{1}{q/c_{p\infty}T_\infty}\left[\frac{\gamma_1(\gamma_\infty-1)}{\gamma_\infty(\gamma_2-1)}\frac{R_1}{R_\infty}\frac{\gamma_2}{\gamma_1}\left(\frac{\gamma_1-1}{\gamma_2-1}\right)^{\frac{\gamma_2-1}{\gamma_2}}\times\left(\frac{\gamma_1 q}{c_{p1}T_1}+1\right)^{\frac{1}{\gamma_2}}\left(\frac{T_1}{T_\infty}\right)^{1-\frac{(\gamma_2-1)\gamma_\infty}{(\gamma_\infty-1)\gamma_2}} - 1\right] \tag{13}$$

(5) Propulsive performance of the engines were obtained in terms of cycle efficiencies, sp. thrust, sp. impulse and TSFC at varying Mach numbers, and plotted for comparison between the baseline and combined-cycle PDTE engine theoretical performances.

4. Results and discussion

With the analysis done as described in the method above, the performance maps for various performance parameters over a range of Mach numbers were established as presented below. The suspended turbofan bypass ratio variation with Mach number is shown in Figure 7. It can be seen that the required bypass decreases to zero near Mach 2.3. Later results show the turbofan performance only up to Mach 2.4, beyond which the baseline turbofan engine performance parameters' values could not be obtained. This shows that the benefits obtained by bypassing the inlet flow in a turbofan engine is no longer valid at higher Mach numbers, hence the use of turbojet engine for a gas-turbine in supersonic fighters. With respect to the present analysis, this result indicates that the turbofan engine is no longer functional and the need for an alternative mode arises. Hence the PDRE takes over as a successive mode of the combined-cycle PDTE.

The performance analysis results indicate that the combined-cycle PDTE outperforms the baseline counterparts in terms of efficiency, sp. thrust, as well as TSFC. Also, as suggested by earlier analytical works on PDEs by Ma et al. [14], the results obtained from the present analysis show that the sp. impulse of the PDRE is higher than the ramjet engine as well as the conventional afterburning turbofan engine. However, the net propulsive gains of combined-cycle PDTE over the baseline engines decrease with Mach number.

4.1. Performance comparison of combined-cycle PDTE in PDA-mode with baseline turbofan engine

The combined-cycle PDTE in PDA-mode is initially set for comparison with the baseline turbofan engine at Mach numbers from 0 to 3. However, the results are only obtained up to Mach 2.4. The analytical comparison results for the sp. thrust and sp. impulse, for the baseline turbofan engine and combined-cycle PDTE, are plotted in Figure 8 and Figure 9, respectively. The sp. impulse of the baseline engine increases with Mach number, but is lower than that of the combined-cycle counterpart. Similarly, the sp. thrust of the baseline engine increases with Mach number as well,

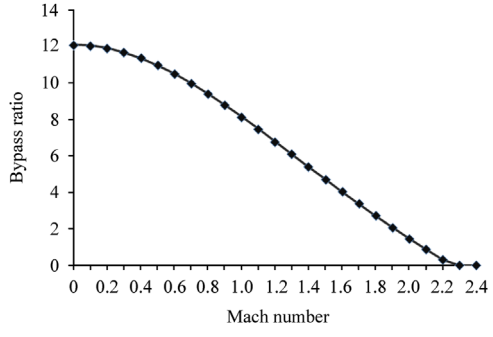

Figure 7 Variation of baseline turbofan bypass ratio with increasing Mach number.

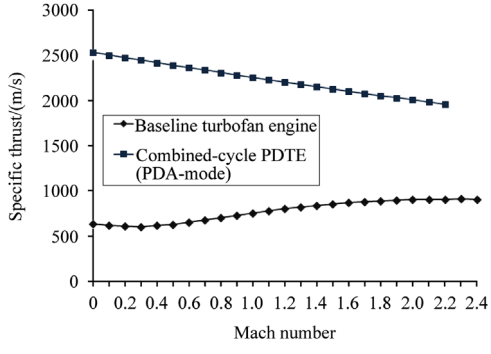

Figure 8 Comparison of sp. thrust variations between baseline turbofan and combined-cycle PDTE (PDA-mode).

while that of combined-cycle PDTE decreases, however it is significantly higher for the later.

The significantly low sp. impulse as well as sp. thrust of the baseline engine in contrast to the known turbofan engines can be attributed to the use of afterburners that consume extra fuel for thrust augmentation, as well as the high-altitude and low density operating conditions.

The TSFC, which is a measure of the propulsive efficiency of an engine, is computed for both the engines at varying Mach numbers. The results are plotted in Figure 10. Notice from Tables 2 and 4 that the fuels used in the baseline afterburner (kerosene) is different from that used in the PDA (hydrogen). The difference in heat of combustion affect, I_{sp} and TSFC values for PDA obtained from Eq. (9) to Eq. (11). The higher value of heat of combustion occurring in the PDA seems to affect the TSFC results in its favor.

Figure 11 compares the cycle efficiencies of the baseline afterburner and the PDA to provide a reasonable basis for the PDA as an alternative to the baseline afterburner. It can be seen that the PDA combustion efficiency is consistently higher than the baseline counterpart. The Humphrey cycle efficiency is seen to be lower but consistently close to that of PDA.

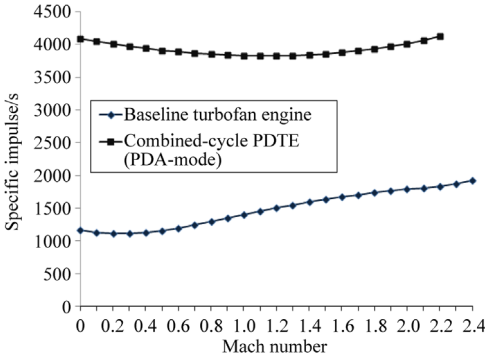

Figure 9 Comparison of sp. impulse variations between baseline turbofan and combined-cycle PDTE (PDA-mode).

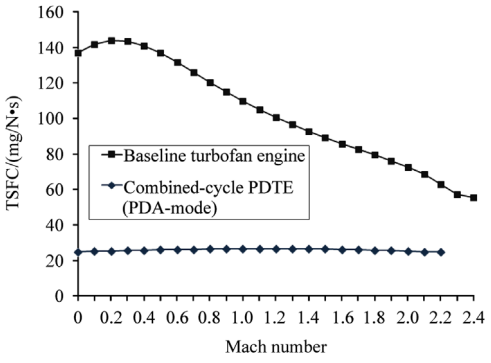

Figure 10 Comparison of TSFC variations between baseline turbofan and combined-cycle PDTE (PDA-mode).

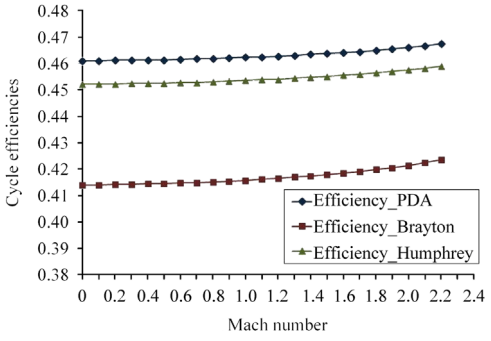

Figure 11 PDA combustion efficiency compared to Brayton cycle efficiency of baseline afterburner, along with that of Humphrey cycle.

4.2. *Performance comparison of combined-cycle PDTE in PDRE-mode with baseline ramjet engine*

The analytical performance results for the sp. thrust and sp. impulse for the baseline ramjet engine and combined-cycle PDTE in PDRE-mode have been plotted in Figure 12 and Figure 13, respectively. As seen in the figures, both sp. thrust and sp. impulse for the baseline ramjet engine become nearly zero near Mach 6, while the PDRE performs very well even at higher Mach numbers. It is interesting to note the variation of PDRE sp. impulse, which decreases steeply as Mach number approaches unity, but increases as

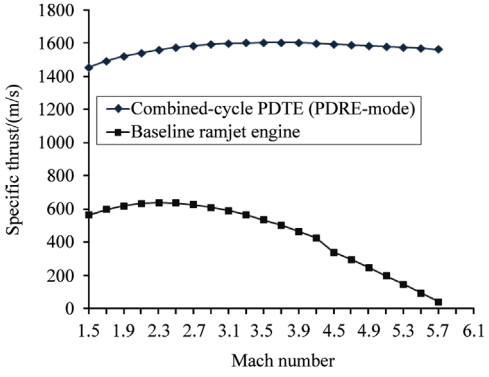

Figure 12 Comparison of sp. thrust variations between baseline turbofan and combined-cycle PDTE (PDRE-mode).

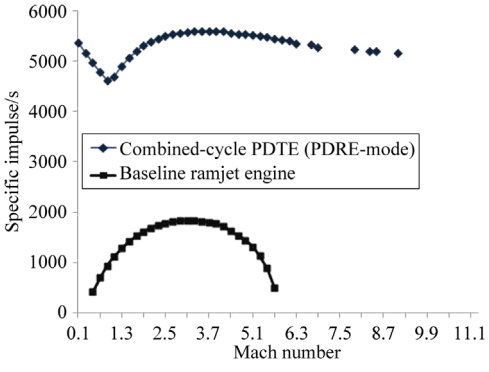

Figure 13 Comparison of sp. impulse variations between baseline turbofan and combined-cycle PDTE (PDRE-mode).

Mach number rises from one. It is caused by the decrease and increase of mass flow through the PDC inlet which is a convergent-divergent-type inlet. Since sp. thrust is independent of mass flow this effect is not observed in its values. Also, PDRE sp. impulse shows operation from zero velocity start-up condition to well above Mach 6 with thoroughly superior performance than the baseline ramjet.

The TSFC of the PDRE and baseline ramjet is compared in Figure 14. The TSFC of PDRE is independent of Mach number, while the ramjet TSFC shows slight improvements as the Mach number increases from 1.5. However, at Mach 5, the TSFC takes a steep incremental turn and the curve becomes almost vertical near Mach 6. The sp. thrust, sp. impulse and TSFC results show that ramjet engines are not practical near Mach 5 and above.

The PDRE combustion efficiency, the Brayton cycle efficiency of the baseline ramjet engine, and the Humphrey cycle efficiency are compared over Mach number in Figure 15. Although he PDRE combustions efficiency is essentially higher at all Mach numbers, as the Mach number approaches 6 all three cycle efficiencies tend to reach similar values. Again, it can be seen that the Humphrey cycle efficiency is significantly close to that of PDRE.

It must be emphasized that different values of heat of combustion of the fuels used in the two engines create dissimilar conditions for their operation which directly affect their performance results. The comparison shows that, for given conditions, the theoretical propulsive efficiency of PDRE is superior to the ramjet engine throughout the Mach range. Also, due to the capability of PDRE to produce static thrust, it has better advantage for low-to-high speed flight application.

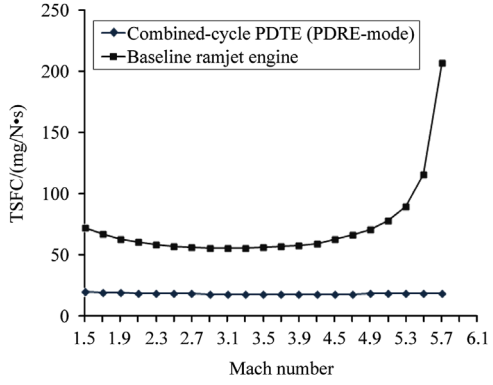

Figure 14 Comparison of TSFC variations between baseline ramjet engine and combined-cycle PDTE (PDRE-mode).

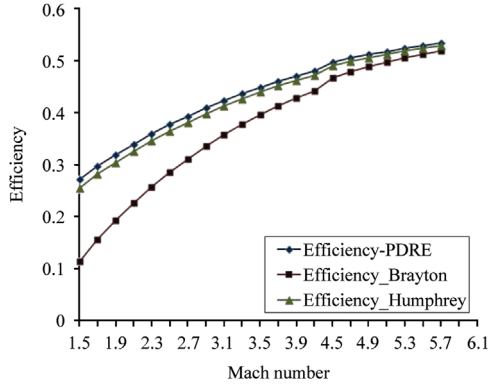

Figure 15 PDRE combustion efficiency compared to that of baseline ramjet engine, along with Humphrey cycle efficiency.

4.3. Performance comparison of combined-cycle PDTE with baseline engine with TIB

The use of turbine inter-vane burner (TIB) in gas-turbine engine has been researched in the past in an attempt to increase the combustion efficiency of the engine by burning the fuel at higher temperature and pressure [16–21]. Apart from the previous comparisons made between performances of the combined-cycle PDTE with baseline turbofan engine, effort was also made to compare the combined-cycle engine's performance with that of the baseline turbofan (afterburning) with TIB and a simple non-afterburning turbofan engine (TF39-GE-1C) with TIB, both burning kerosene as fuel.

Table 5 Configuration details for various engines analyzed.

Engine	Components			
	Conventional afterburner	Ram duct	Pulse detonation afterburner	Turbine inter-vane burner
TF39-GE-1C Baseline engine	√	√		
Combined-cycle PDTE		√	√	
Baseline engine with TIB	√	√		√
Turbofan engine with TIB				√

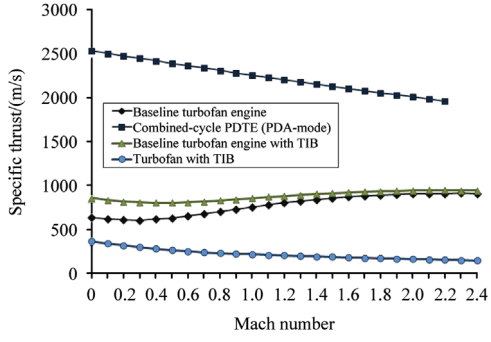

Figure 16 Comparison of sp. thrust for combined-cycle PDTE (PDA-mode), baseline with and without TIB and non-afterburning turbofan with TIB.

The baseline engine high-pressure turbine stage was accommodated with TIB and its performance calculated at increasing Mach numbers ranging from 0 to 2.4. Similarly, performance calculation was also done for a non-afterburning turbofan engine accommodated with TIB at the high-pressure turbine. To avoid the ambiguity about the components used in engine configurations discussed and analyzed so far, the component-wise classification of the engine configurations is presented in Table 5.

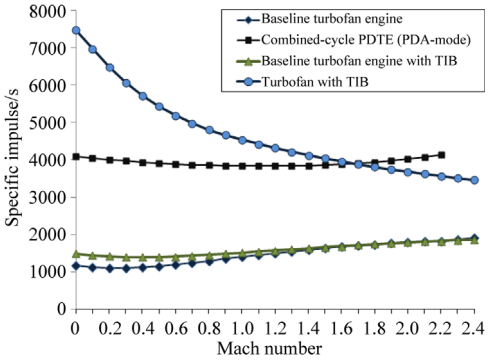

Figure 17 Comparison of sp. impulse for combined-cycle PDTE (PDA-mode), baseline with and without TIB and non-afterburning turbofan with TIB.

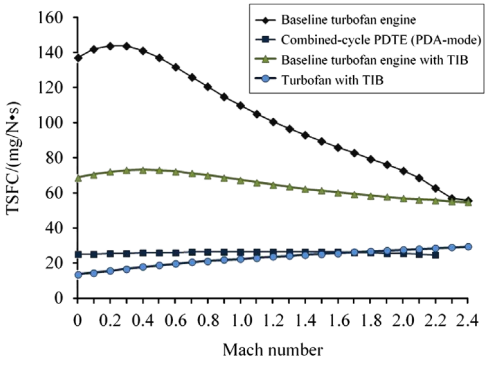

Figure 18 Comparison of TSFC for combined-cycle PDTE (PDA-mode), baseline with and without TIB and non-afterburning turbofan with TIB.

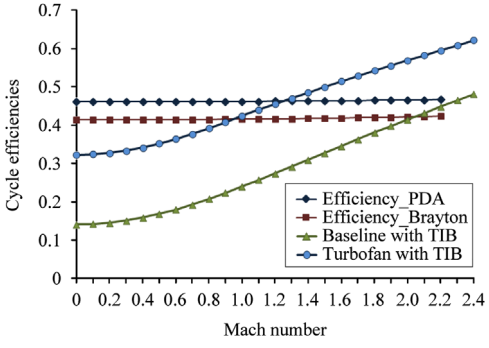

Figure 19 Overall combustion cycle efficiency comparison for combined-cycle PDTE (PDA-mode), baseline with and without TIB and non-afterburning turbofan with TIB.

The performance results for combined-cycle engine, baseline engine, baseline engine with TIB, and turbofan engine with TIB have been plotted in Figure 16 to Figure 19 for comparison. The results clearly show the performance gain of using TIB in the baseline engine, especially in terms of TSFC at lower Mach numbers. While in terms of sp. thrust and sp. impulse, the improvements do not seem substantial. More importantly, the baseline engine accommodated with TIB does not meet the performance superiority of the combined-cycle engine operating with a PDA in terms of the first three parameters. However, the use of TIB seems to have positive effects on the cycle efficiency for the baseline engine, as well as for the turbofan engine without afterburner.

5. Conclusions

(1) In this study, analytical models of baseline turbofan engine, baseline ramjet engine and combined-cycle PDTE at PDA and PDRE modes were created. An analytical method was devised for computation of theoretical propulsive performances of the above engines at varying Mach numbers.

(2) The performance analysis verified the theoretical claims that the propulsive performance of a gas-turbine can be greatly improved by replacing the conventional afterburner with a PDA. The efficiency of a constant volume PDA is higher than conventional constant pressure deflagration afterburners throughout the analyzed Mach range (Mach 0 to Mach 6).

(3) The claims that by the use of PDA, the sp. thrust of the new PDTE concept can nearly be twice as much as those of the conventional afterburning turbofan engine has been verified. Also, the TSFC of PDTE is significantly less than the conventional counterpart. However, the net propulsive gain decreases with increasing Mach number.

(4) The PDRE also outperforms its ramjet counterpart for all flight conditions considered herein; the gains obtained in specific thrust, specific impulse and TSFC are outstanding.

(5) If a PDRE is provided with some mechanism to provide airflow at the start-up phases, it can show excellent propulsive performance. This creates the necessity of combining gas-turbine engines with PDEs, since the turbine engines can provide the necessary airflow to the integrated system.

(6) Here, it is important to stress the fact that if the hydrogen fuel, used in pulse detonating configurations, was also used in the conventional counterparts, the propulsive performance of both the turbofan engine and the ramjet engine can greatly improve, specially the sp. impulse. The improved sp. impulse of combined-cycle PDTEs is very substantial both in terms of its increased value and the extended operational range.

(7) In a separate analysis, the baseline turbofan engine was accommodated with TIB and its performance compared with the original baseline turbofan engine, the combined-cycle PDTE at PDA-mode, and a simple turbofan engine with TIB. The comparisons indicate substantial benefits of the combined-cycle PDTE over the concept of TIB in gas-turbine engines over a wider range of Mach numbers.

(8) This study presents a theory-based performance analysis of the combined-cycle PDTE concept under idealized conditions. Further computational as well as numerical work needs to be carried out for all modes of operation of the combined-cycle PDTE concept, with better consideration of the associated physical mechanism and the combustion phenomena, to fully understand and verify the potentials they hold over the other propulsion systems considered in this study.

Acknowledgement

This work was supported by the National Natural Science Foundation of China (NSFC No. 50776045, 51076064), and China Scholarship Council's International Students Scholarship (CSC No. 2011YXS867) from the Minister of Education, China and NUAA.

References

[1] T.R.A. Bussing, G. Pappas, Pulse detonation engine theory and concepts, in: S.N.B Murthy, E.T. Curran (Eds.), Developments in High-Speed Vehicle Propulsion Systems, Vol. 165, Progress in Aeronautics and Astronautics, AIAA, Reston, VA, 1996, pp. 421–472.

[2] K. Kailasanath, Applications of detonations to propulsion: a review, AIAA Paper 99–1067, January 1999.

[3] K. Kailasanath, Review of propulsion applications of detonation waves, AIAA Journal 38 (9) (2000) 1698–1708.

[4] C.R. Thorn, Off-design analysis of a high-bypass turbofan engine using a pulsed detonation combustor, Master Dissertation, Air Force Institute of Technology, AFIT/GAE/ENY/10-M26, March 2010.

[5] M.A. Mawid, T.W. Park, B. Sekar, Performance analysis of a pulse detonation device as an afterburner, in: 36th AIAA/ASME/SAE/ASEE Joint Propulsion Conference and Exhibit, Huntsville, U.S., July 16-19, 2000, AIAA 2000-3474.

[6] M.A. Mawid, T.W. Park, Towards replacement of turbofan engine afterburners with pulse detonation devices, AIAA 2001-3470, 2001.

[7] M. Lam, D. Tillie, T. Leaver, B. McFadden, Pulse detonation engine technology: an overview, Applied Science 201, University of British Columbia, November 26, 2004.

[8] M.A. Mawid, T.W. Park, B. Sekar, C. Arana, Application of pulse detonation combustion to turbofan engines, Journal of Engineering for Gas Turbines and Power 125 (1) (2003) 270–283.

[9] J.E. Johnson, L.W. Dunbar, L. Butler, U.S. Patent Application for a "Combined-Cycle Pulse Detonation Engines," US 6,666,018 B2, filed 23 Dec. 2003.

[10] J.E. Johnson, L.W. Dunbar, L. Butler, U.S. Patent Application for a "Combined-Cycle Pulse Detonation Turbine Engines," US 6,442,930 B1, filed 3 Sep. 2002.

[11] J.E. Johnson, L.W. Dunbar, L. Butler, U.S. Patent Application for a "Combined-Cycle Pulse Detonation Engines," US 6,550,235 B2, filed 22 Apr. 2003.

[12] AEDsys Software Suite URL:⟨http://www.aircraftenginedesign.com/custom1.html2.html⟩.

[13] W.H. Heiser, D.T. Pratt, Thermodynamic cycle analysis of pulse detonation engines, Journal of Propulsion and Power 18 (1) (2002) 68–76.

[14] F. Ma, J.Y. Choi, V. Yang, Propulsive performance of airbreathing pulse detonation engines, Journal of Propulsion and Power 22 (6) (2006) 1195–1196.

[15] I.Q. Andrus, Comparative analysis of a high-bypass turbofan engine using a pulsed detonation combustor, Master Thesis, Air Force Institute of Technology, AFIT/GAE/ENY/07-M02, 2007.

[16] T.V. Moe, H. Tang, A. Carrere, Numerical investigation of turbine inter-blade (TIB) concepts with two different radial vane cavity shapes, in: Nanjing 7th International Conference on Computational and Experimental Engineering and Sciences, 2011, ICCES1120101227112.

[17] T.V. Moe, Numerical investigation of ultra-compact combustor models for turbine inter-blade burner (TIB), Nanjing University of Aeronautics and Astronautics, Nanjing, 2011.

[18] M. Li, H. Tang, C. Zhang, B. Cheng, D. Mo, Numerical simulation of a novel turbine inter-vane burner, Journal of Aerospace Power 27 (1) (2012) 55–62.

[19] M. Li, H. Tang, D. Mo, C. Zhang, Numerical simulation of influence of equivalence ratio on turbine inter-vane burner, Journal of Combustion Science and Technology 18 (2) (2012) 161–168.

[20] D. Mo, H. Tang, M. Li, H. Zheng, Numerical simulation of turbine inter-blades burner (TIB) with different axial cavity shapes, Aeroengine 38 (1) (2012) 33–36.

[21] B. Cheng, H. Tang, X. Xu, X. Li, Performance study on turbofan engine with turbine inter burner, Aeroengine 36 (6) (2010) 18–22.